J Therm Anal Calorim (2009) 98:355–360
DOI 10.1007/s10973-009-0289-8

Influence of pH on nanosized Mn–Zn ferrite synthesized by sol–gel auto combustion process

H. Waqas · A. H. Qureshi

Received: 13 October 2008 / Accepted: 18 February 2009 / Published online: 6 August 2009

Abstract Sol–gel auto combustion process was employed to synthesize nanosized Mn–Zn ferrite at different pH values (<1, 5, 6, 7, 8 and 10). Although self propagating combustion behavior of gel was noted at pH 5 but more effective combustion was observed at pH 6. The smoldering effect was observed in gel prepared at pH 7, 8 and 10, whereas pH < 1 showed localized burning. Thermogravimetric (TG) and X-ray diffraction (XRD) analyses were done to investigate the effect of pH on the combustion behavior, particle size and the formation of desired magnetic (spinel) phase. From TG curves of burnt powders, activation energy of ignition reaction at each pH value was calculated. The results showed that fuel to oxidant ratio and the amount of gel residuals decided the value of activation energy required to further purify the burnt powders. Calcination parameters (time and temperature in air) of powders P1 and P6 synthesized at pH < 1 and pH 6 were also determined. B–H loop results showed that calcined powder C6 was more ferromagnetic than C1 due to fully developed spinel phase and larger particle size.

Keywords Activation energy · FTIR study · Mn–Zn ferrite · Sol–gel auto combustion · VSM · XRD study

H. Waqas (✉)
Department of Chemical and Materials Engineering, PIEAS, P.O.Nilore, Islamabad, Pakistan
e-mail: hw_pk@yahoo.com

A. H. Qureshi
Materials Division, Directorate of Technology, PINSTECH, Islamabad, Pakistan

Introduction

Mn–Zn ferrite (MZF) is very important class of soft ferrites. It has many applications in the filed of electronics. These can be used as deflection yoke rings, antenna rods, electromagnetic interference suppressors, core materials for electronic transformers etc. [1–3]. From crystallographic point of view it has spinel structure. The major unit cell of spinel lattice is composed of eight sub unit cells having face centre cubic (FCC) geometry. Further more there are total 64 tetrahedral and 32 octahedral interstitial sites available within each unit cell. Chemically spinels are denoted by (MO. Fe_2O_3) where 'MO' refers to a combination of two or more divalent metal oxides e.g. oxides of iron, nickel, manganese, zinc etc. The addition/substitution of divalent oxides occupied the tetrahedral or octahedral sites in such a manner that the total charge on spinel lattice becomes neutral. This inherent property of charge balance classified spinel as normal, inverse or mixed spinels [3]. It has been observed [4–6] that all the issues related to charge balance, site occupancy and electrical & magnetic properties of MZF depend upon the adopted synthesis route. Different synthesis routes like ball milling [7–9], sol–gel [10, 11], sol–gel auto combustion [12, 13], coprecipitation [14], hydrothermal [15], thermal decomposition technique [16], novel hydrazine method [17], polymeric precursor method [18, 19] etc. are being used to prepare soft ferrite powders. Each method has its own advantages and limitations on the properties of synthesis product. Sol–gel auto combustion process is one of the well known techniques to produce nanosize powders. The self propagating combustion process not only helped to eliminate the unwanted species like water content and organic molecules (–COOH) but also lower down the calcination temperature. In this method pH of the

initial solution, fuel to oxidant ratio and the purity of metallic salts are very important [12, 13].

In present research, nanosized Mn–Zn ferrite has been synthesized by sol–gel auto combustion process. The effect of pH on combustion behavior, thermal decomposition of gel/powder has been studied and optimized. The activation energy [20, 21] required to further purify the burnt powders (powder obtained after ignition of gel) have also been calculated. The calcination temperature for the burnt powders synthesized at pH < 1 and 6 have been studied and optimized. The magnetic properties like coercivity (H_c), remonance (B_r) and saturation magnetization (M_s) of the calcined powders have also been discussed in relation with calcination parameters.

Experimental

Sol–gel auto combustion process was employed to synthesize Mn–Zn ferrite system having composition of $Mn_{0.57}$ $Zn_{0.35}$ $Fe_{2.08}$ $O_{4\pm\delta}$. Nitrates (iron, manganese, zinc) and citiric acid of Analar Grade with high purity (99.99%) were used as starting materials. The solution of these nitrates was prepared by dissolving in demineralized water (DMW). To chelate the metal ions, citric acid (1:1 molar ratio with respect to metal ions) was also added. This initial solution was highly acidic and having pH < 1. Ammonia was added to adjust different pH values (5, 6, 7, 8 and 10) of the initial solution. These solutions were evaporated at 75 °C to get dry gel. Upon further heating at temperature around 220 °C self propagating combustion/ignition reaction was started within the gel and the whole gel was converted into burnt powder in each case. The samples against each pH values were designated as P1, P5, P6, P7, P8 and P10.

Thermal decomposition behaviors of the gel/powders were studied by simultaneous thermal analyzer (NETZSCH-409) with heating rate of 10 °C/min in the presence of air. Fourier transform infrared (FTIR) spectroscopy (Variance-3100) was employed to investigate the presence of different functional groups (NO_3, –COOH, –OH) and metal oxide (M–O) in burnt powders. Activation energies of burnt powder samples P1, P5, P6, P7, P8 and P10 were calculated from mass loss curves. The phase study was done by using X-ray diffraction (XRD) with Cuk_α radiation $\lambda = 1.5406$ Å (Bruker D-5005). The data was collected in 2θ range from 20 to 75 degree with a scan rate of 0.02 degree/sec. B–H loops of calcined powders C1 (P1 designated after calcination) and C6 (P6 designated after calcination) were measured by vibrating sample magnetometer (VSM) system (Lakeshore-3500) at room temperature.

Results and discussion

Formation of burnt powders

It was observed that self propagating combustion/ignition behavior of the dry gel strongly influenced by pH of the initial solution. Actually, fuel to oxidant ratio (citric/ammonia) plays crucial role in the combustion of gel. This ratio can be changed by varying the pH of the initial solution with addition of ammonia. In this research, gel prepared at pH 6 showed complete combustion among all other gel prepared at pH (<1, 5, 7, 8 and 10). Thermogravimetric analysis (TGA) for the gel prepared at pH 6 is shown in Fig. 1. From this figure it can be observed that after the evaporation of water content from gel, self propagating combustion (exothermic reaction) was started at 220 °C and almost 80% of the initial mass was lost in form of water and evolved gases like CO_2, CO, NO_2 etc. Hence fully crystalline fluffy powder (P6) was obtained at the end of combustion process for pH 6, Fig. 2a–b. In case of pH 5, the self propagation ignition was also observed but its rate was a bit lower than pH 6 therefore the intensity of spinel phase in P5 burnt powder was lower than P6. The

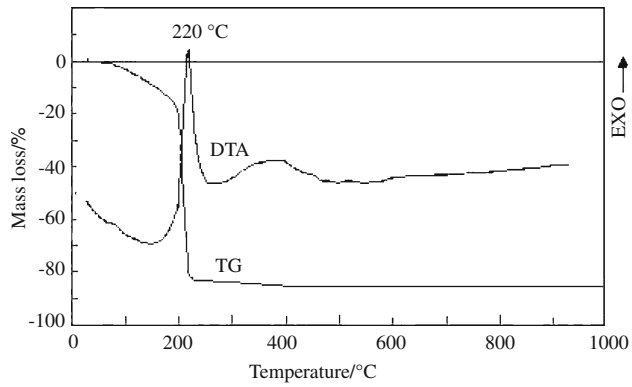

Fig. 1 TG/DTA curves of Mn–Zn Ferrite gel prepared at pH 6

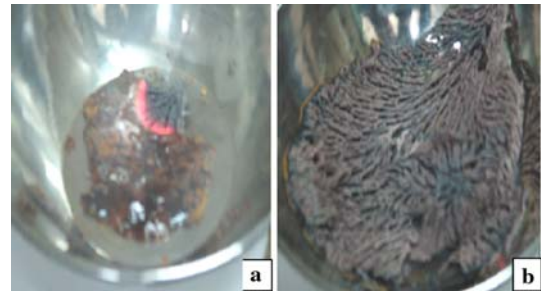

Fig. 2 Self propagating combustion behavior of gel prepared at pH 6. **a** Initiation of combustion, **b** Fluffy powder obtained at the end of combustion process

gel prepared without addition of ammonia (pH < 1) ignited in a localized manner (i.e. no self propagating combustion) and high density amorphous powder was obtained. However the gel prepared at higher pH (7, 8 and 10) showed smoldering behavior (partial combustion with emission of ammonia rich fumes) during combustion. It revealed that the excess ammonia in solutions having pH 7, 8 and 10 prevented the process of spontaneous ignition therefore partially burnt powders were obtained at these pH values. These results exposed that fuel to oxidant ratio in the initial solution should be optimum to obtain fully crystalline fluffy powder at low temperature i.e. around 220 °C.

Analyses of burnt powders

Thermogravimetry (TG) was carried out for burnt powder samples P1, P5, P6, P7, P8 and P10 and their normalized mass loss curves are shown in Fig. 3. TG curves showed that each sample again lost some of its mass during heating. The total mass loss of each burnt powder during the TG test was plotted against its pH value as shown in Fig. 4.

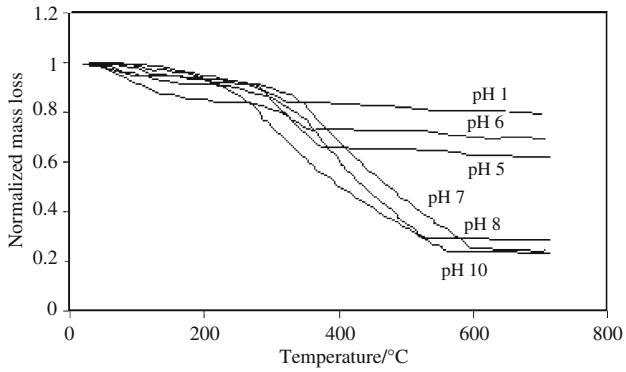

Fig. 3 Normalized mass loss curves of burnt powder samples (P1 < 1, P5, P6, P7, P8 and P10)

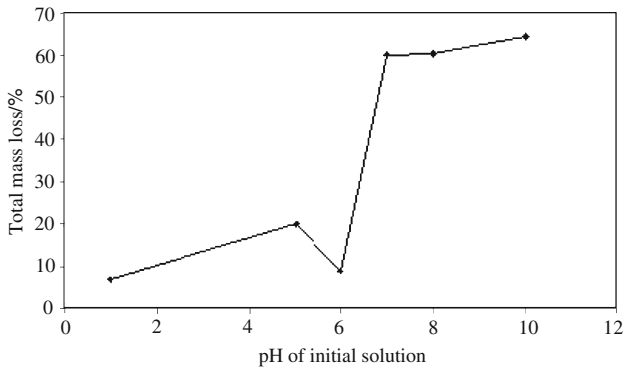

Fig. 4 pH of the initial solution versus total mass loss (%) of burnt powder samples (P1 < 1, P5, P6, P7, P8 and P10) during heating

This mass loss can be attributed due to the removal of residuals (gel particulates, ammonia and trapped gases) from burnt powders during heating. The figure clearly shows that mass loss for each powder is directly related with its combustion behavior followed during synthesis. The burnt powder P6 has minimum mass loss than others because of taking the advantage of highest combustion rate during its synthesis. Similarly the mass loss response for other powders P1, P5, P7, P8 and P10 can be justified on the basis of their combustion behaviors.In order to further clarify the concept of pH dependent ignition response, activation energy for each burnt powder was calculated from its normalized mass loss curve. The slope of normalized mass loss curve was used to find out activation energy for the residual burning of each burnt powder according to Eq. 1.

$$\ln \ln[(W_o - W_t^f)/(W_t - W_t^f)] = E^*\theta/RT_s^2 \quad (1)$$

where W_t is the mass remaining at given temperature, W_o and W_t^f are initial and final mass respectively, E^* is the activation energy, θ is the temperature, R is universal gas constant and T_s is reference temperature.

The order of reaction (n) was assumed to be one. The detailed explanation of this method is in given in references [20, 21].

The relation between pH value and the calculated activation energy is shown in Fig. 5. It was observed that minimum activation energy was required to start the combustion process within the powders prepared at pH 7, 8 and 10. The reason for this behavior is clear, for basic solutions the content of ammonia was higher than optimum amount, therefore burnt powder still have some trapped ammonia that again reacted with unburned nitrate complexes and helped to ignite the powders during heating. Whereas, maximum value of activation energy was observed for the sample (P1). As no ammonia was added in the initial solution of P1 therefore high energy was required

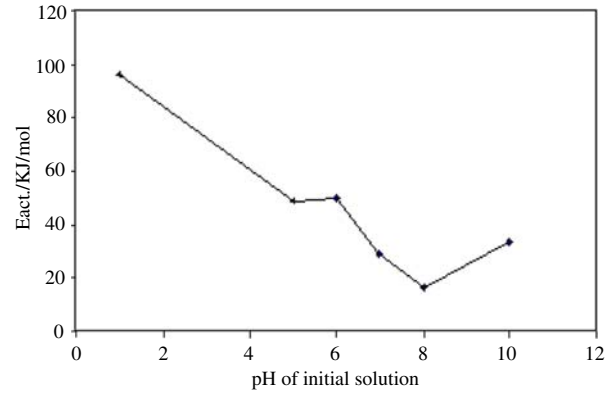

Fig. 5 Activation energy of burnt powder samples (P1 < 1, P5, P6, P7, P8 and P10)

to completely burnt the nitrate-citrate complex. While powders synthesized at pH 5 and 6 were almost fully burnt during gel heating therefore intermediate values (48.07 and 50.16 KJ/mol) of activation energies were noted for them. These calculated activation energies closely matched with the values reported in literature for the thermal decomposition of nitrate complexes [22, 23]. Therefore, it can inferred that the rate of activation energy essentially effected by pH of the initial solution.

FTIR analysis was also employed to verify the presence of residuals in the burnt powders of samples P1, P5, P6, P7, P8 and P10 as shown in Fig. 6a–f. As discussed earlier that powder synthesized at 7, 8 and 10 pH values still have some excess amount of nitrate and ammonia ions. Their presence was confirmed by pointing out the larger peaks at 1,386 cm^{-1} and 1,556 cm^{-1} positions in the FTIR spectrum [24]. However in case of sample P6, no peaks of ammonia or nitrates ions were noted at the above mentioned wave numbers while stronger peaks of metal oxide (spinel phase) [25] were observed at 470 cm^{-1} and 535 cm^{-1} positions as shown in Fig. 6c. It confirmed that gel prepared at pH 6 was highly burnt during the combustion process and fluffy powder was obtained with fully developed spinel phase. For sample P1, FTIR spectra clearly showed the peaks of unburnt nitrates at 1,386 cm^{-1} and carbonyl compounds $\sim$2,360 cm^{-1}. It confirmed that only localized burning has occurred without the presence of oxidant (ammonia) that helps to start high temperature self propagation reaction. So, FTIR spectrums also confirm that the formation of spinel phase at low temperature is more favorable in P6 (pH 6) than all other samples (P1, P5, P7, P8 and P10).

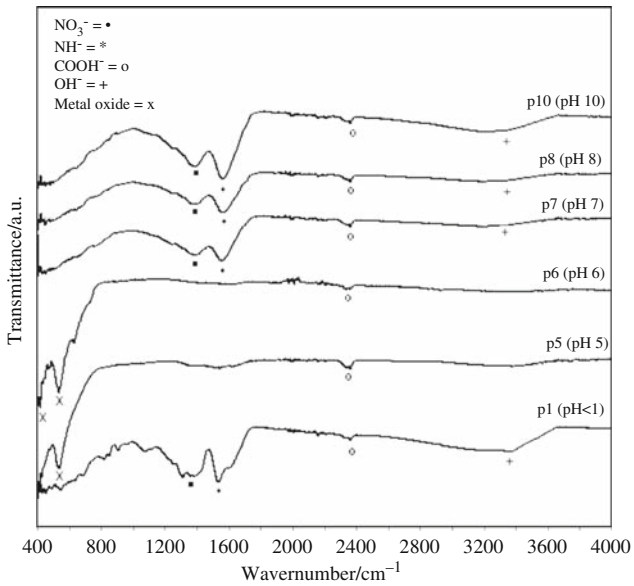

Fig. 6 FTIR analysis of burnt powder samples P1, P5, P6, P7, P8 and P10

Therefore the results of activation energy can also be justified on the basis of FTIR spectrum analysis as described above.

Calcination studies

Calcination is mainly conducted to remove the un-burnt volatile species and to avoid the shrinkage process during sintering [24].

Figure 7 shows XRD patterns of burnt powders (P1, P5, P6, P7, P8 and P10) synthesized at pH (<1, 5, 6, 7, 8 and 10) by sol–gel auto combustion process. The spinel lattice was observed for the powders P5 and P6 but XRD peaks for spinel phase were more clear and fully developed for pH 6. It showed that optimum combustion condition has obtained for pH 6. Whereas, partially crystalline or amorphous patterns were observed for P1, P7, P8 and P10 samples.

P1 and P6 samples were selected to study the effect of pH on calcination. As sample P6 had already fully developed spinel lattice therefore there was no need of high temperature for calcination. It was just kept at 450 °C for 20 min to purifying the powder. Figure 8 shows the XRD pattern of calcined sample C6. Approximately 25 ± 3 nm particle size was obtained by employing Scherrer formula. Whereas the sample P1 synthesized at pH < 1 (no ammonia addition) was almost amorphous. This sample (P1) was calcined in the temperature range of 300 °C to 700 °C to determine the optimum calcination conditions. It was observed that although the spinel phase was formed by heating the powder at 300 °C followed by 700 °C for different intervals of time but the problem of non magnetic phase (Fe_2O_3) was aroused. This problem was resolved by heating the burnt powder only at 700 °C for 60 min in air. In this case the single phase (spinel) and particle size of 7 nm ± 3 nm were obtained. Figure 9 shows XRD

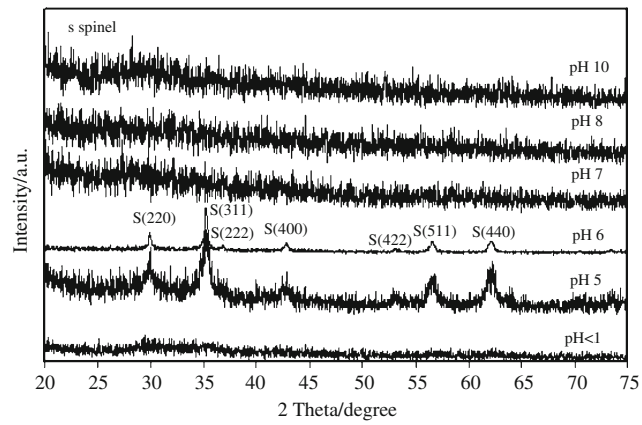

Fig. 7 XRD patterns of burnt powders synthesized at pH < 1, 5, 6, 7, 8 and 10

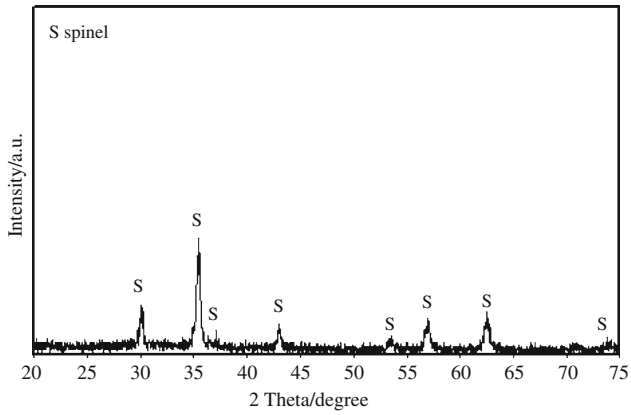

Fig. 8 XRD pattern of sample (C6) calcined at 450 °C, 20 min

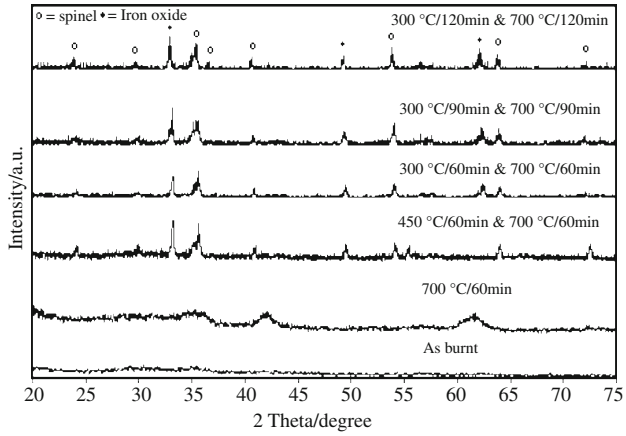

Fig. 9 XRD patterns of sample (C1) calcined at different times and temperatures

spectrums of C1 sample obtained at different calcination conditions. From this study it can be inferred that calcination parameters i.e. temperature and time for sol–gel auto combustion process indirectly depend upon the pH value of the initial solution.

Hysterisis loop

B–H loops of the samples C1 (calcined at 700 °C for 60 min) and C6 (calcined at 450 °C for 20 min) are shown in Fig. 10. These loops showed that C6 was more ferromagnetic than C1. The magnetic properties such as coercivity (H_c), remonance (B_r) and saturation magnetization (Ms) of C6 are quite high as compared to C1 as shown in Fig. 10. The adequate ferromagnetic behavior of C6 was due to the formation of complete spinel phase and the growth of particles during the auto combustion and calcination processes respectively. Whereas for the sample C1, the powder obtained after ignition and calcination had particle size less than 10 nm. According to study [25, 26]

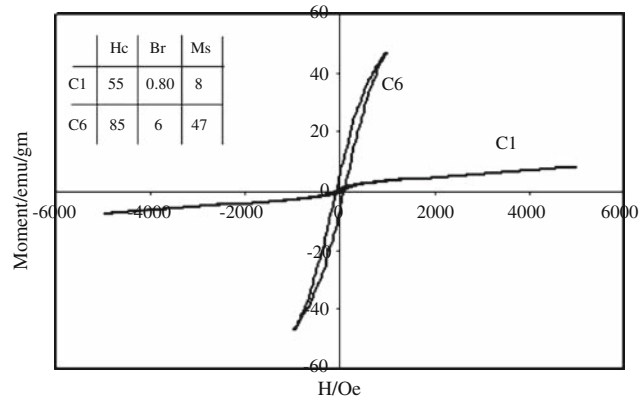

Fig. 10 B–H loop properties of calcined samples C1 and C6

magnetic particles less than 10 nm showed superparamagnetic behavior. However, C1 was not showing superparamagnetism due to retaining some ferromagnetism ($H_c \neq 0$). These results revealed that the rate of combustion and calcination conditions strongly influenced the magnetic properties of nanosized Mn–Zn ferrite synthesized by sol–gel auto combustion process.

Conclusions

pH of initial solution plays a significant role to synthesize nanosized Mn–Zn ferrites by sol–gel auto combustion process. Activation energy required to start auto combustion can be decreased by optimizing the fuel to oxidant ratio. Magnetic properties of nanosized Mn–Zn ferrite strongly influenced by processing and calcination conditions.

Acknowledgements Authors would like to thank Pakistan Higher Education Commission (HEC) for providing financial assistance.

References

1. Arulmurugan R, Vaidyanathan G, Sendhilnathan S, Jeyadevan B. Mn–Zn ferrite nanoparticles for ferrofluid preparation: study on thermal–magnetic properties. J Magn Mag Mater. 2006;298:83–94.
2. Levy D, Hoser A. Cation distribution in synthetic zinc ferrite ($Zn_{0.97}Fe_{2.02}O_4$) from in situ high-temperature neutron powder diffraction. Am Mineral. 2000;85:1497–502.
3. Tangsali RB, Keluskar SH, Niak GK, Budkuley JS. Effect of sintering conditions on resistivity of nanoparticle Mn–Zn ferrite prepared by nitrilotriacetate precursor method. J Mater Sci. 2007;42:878–82.
4. Ahns SJ, Yoon CS, Yoon SG, Kim CK, Byun TY, Hong KS. Domain structure of polycrystalline MnZn ferrites. Mater Sci Eng B. 2001;84:146–54.
5. Parekh K, Upadhyay RV, Belova L. Ternary monodispersed $Mn_{0.5}Zn_{0.5}Fe_2O_4$ ferrite nanoparticles: preparation and magnetic characterization. Nanotechnology. 2006;17:5970–5.
6. Botta PM, Bercoff PG, Aglietti EF, Bertorello HR, Lopez JMP. Two alternative synthesis routes for Mn–Zn ferrites using mechanochemical treatments. Ceram Inter. 2006;32:857–63.

7. Rosales MI, Plata AM, Nicho ME, Brito A, Ponce MA. Effect of sintering conditions on microstructure and magnetic properties of Mn–Zn ferrites. J Mater Sci. 1995;30:4446–50.
8. Ding J, McCormick PG, Street R. Formation of spinel Mn–ferrite during mechanical alloying. J Magn Mag Mater. 1997;171:309–14.
9. Qureshi AH. The influence of hafnia and impurities (CaO/SiO_2) on the microstructure and magnetic properties of Mn–Zn ferrites. J Cryst Growth. 2006;286:365–70.
10. Azadmanjiri J. Preparation of Mn–Zn ferrite nanoparticles from chemical sol–gel combustion method and the magnetic properties after sintering. J Non Cryst Solids. 2007;353:4170−3.
11. Mandal K, Mandal SP, Agudo P, Pal M. A study of nanocrystalline (Mn–Zn) ferrite in SiO_2 matrix. Appl Surf Sci. 2001;182:386–9.
12. Azadmanjiri J, Seyyed Ebrahimi SA. The effect of pH and citric acid concentration on the characterization of nanocrystalline $NiFe_2O_4$ powder synthesized by a sol–gel autocombustion method. Phys Metals Metallogr. 2006;102:S21–3.
13. Azadmanjiri J, Salehani HK, Barati MR, Farzan F. Preparation and electromagnetic properties of $Ni_{1-x}Cu_xFe_2O_4$ nanoparticle ferrites by sol–gel auto-combustion method. Mater Lett. 2007;61:84–7.
14. Zhang ZJ, Wang ZL, Chakoumakos BC, Yin JS. Temperature dependence of cation distribution and oxidation state in magnetic Mn−Fe ferrite. J Am Chem Soc. 1998;120:1800–4.
15. Wang H, Kung S. Crystallization of nanosized Ni–Zn ferrite powders prepared by hydrothermal method. J Magn Mag Mater. 2004;270:230–6.
16. Wang XH, Li XJ, Yan HH, Qu YD, Sun GL, Xie XH, et al. Research on thermal decomposition kinetic characteristic of emulsion explosive base containing Fe and Mn elements. J Therm Anal Calorim. 2008;91:545–50.
17. Rane KS, Uskaikar H, Pednekar R, Mhalsikar R. The low temperature synthesis of metal oxides by novel hydrazine method. J Therm Anal Calorim. 2007;90:627–38.
18. Xavier CS, Candeia RA, Bernardi MIB, Lima SJG, Longo E, Paskocimas CA, et al. Effect of the modifier ion on the properties of $MgFe_2O_4$ and $ZnFe_2O_4$ pigments. J Therm Anal Calorim. 2007;87:709–13.
19. Silva MRS, De Miranda LCO, Cassia-Santos MR, Lima SJG, Soledade LEB, Longo E, et al. Influence of the network former on the properties of magnesium spinels. J Therm Anal Calorim. 2007;87:753–7.
20. Horowitz HH, Metzger G. A new analysis of thermogravimetric traces. Anal Chem. 1963;35:1465–8.
21. Zyrichev NA, Shlenskii OF. Kinetics of decomposition of hydrated nitrates by short contact time plasma heating. High Energy Chem. 2000;34:46–52.
22. Singh G, Singh CP, Frohlich R. Preparation, characterization and thermolysis of metal nitrate complexes with 4,4′-bipyridine. J Therm Anal Calorim. 2006;85:425–31.
23. Singh G, Baranwal BP, Kapoor IPS, Kumar D, Singh CP, Frohlich R. Transition metal nitrate complexes with hexamethylenetetramine. J Therm Anal Calorim. 2008;91:971–7.
24. Qureshi AH, Arshad M, Durrani SK, Waqas H. Impact of Pb substitution on the formation of high T_c superconducting phase in BSCCO system derived through sol–gel process. J Therm Anal Calorim. 2008;94:175–80.
25. Tomar MS, Singh SP, Perez OP, Guzman RP, Calderonc E, Ramo CR. Microelectron synthesis and magnetic behavior of nanostructured ferrites for spintronics. Microelectron J. 2005;36:475–9.
26. Makovec D, Kodre EA, Arcon I, Drofenik M. Non-stoichiometric zinc–ferrite spinel nanoparticles. J Nanopart Res. 2008;10:131–41.